

## 2 Model Description

---

### Governing Equations

Fluid motion is modeled using the 2-D unsteady shallow-water equations. The shallow-water (or long-wave) equations are a result of the vertical integration of the equations of mass and momentum conservation for incompressible flow under the hydrostatic pressure assumption. This assumption implies that vertical accelerations are negligible when compared to the horizontal accelerations and the acceleration due to gravity. The vertical accelerations are small when the characteristic wavelength is long relative to the depth, which is why these equations are referred to as long-wave or shallow-water equations. The drawdown wave is on the order of the length of the barge train, which is much greater than the channel depth. Vertical accelerations, which result from streamline curvature, reduce the celerity of a gravity wave by the ratio (Whitham 1974):

$$K = \left\{ 1 + \left( \frac{4\pi^2 h^2}{3L^2} \right) \right\}^{-1/2} \quad (1)$$

where  $h$  is the flow depth and  $L$  is the wavelength. For the test cases presented in this report, the wavelength is approximately 10 m and the generated wave (drawdown) is about 0.2 m. Therefore,  $K$  equals 0.9974, which means that the computed wave speed is only 0.26 percent larger than wave speeds in the real system. Near the vessel the horizontal accelerations are greater, which in turn suggests that pressure gradients and vertical accelerations are more important. Although non-negligible vertical accelerations are present in the immediate vicinity of the vessel, the hydrostatic assumption is reasonable for the flow at some distance away from the vessel, which is the interest in this study.

The dependent variables of the fluid motion are defined by the flow depth  $h$ , the  $x$ -component of unit discharge  $p$ , and the  $y$ -component of unit discharge  $q$ . These dependent variables are functions of the two space directions  $x$  and  $y$  and time  $t$ . If the fluid pressure at the surface is included while the free-surface stresses are neglected, the shallow-water equations are given as (Abbott 1979):

$$\frac{\partial U}{\partial t} + \frac{\partial F}{\partial x} + \frac{\partial G}{\partial y} + \mathbf{H} = \mathbf{0} \quad (2)$$

where

$$\mathbf{U} = \begin{Bmatrix} h \\ p \\ q \end{Bmatrix} \quad (3)$$

$$\mathbf{F} = \begin{Bmatrix} p \\ \frac{p^2}{h} + \frac{1}{2}gh^2 - h \frac{\sigma_{xx}}{\rho} \\ \frac{pq}{h} - h \frac{\sigma_{yx}}{\rho} \end{Bmatrix} \quad (4)$$

$$\mathbf{G} = \begin{Bmatrix} p \\ \frac{pq}{h} - h \frac{\sigma_{xy}}{\rho} \\ \frac{q^2}{h} + \frac{1}{2}gh^2 - h \frac{\sigma_{yy}}{\rho} \end{Bmatrix} \quad (5)$$

and

$$\mathbf{H} = \begin{Bmatrix} 0 \\ gh \frac{\partial z_0}{\partial x} + \frac{h}{p} \frac{\partial P}{\partial x} + n^2 g \frac{p \sqrt{p^2 + q^2}}{C_o^2 h^{7/3}} \\ gh \frac{\partial z_0}{\partial y} + \frac{h}{p} \frac{\partial P}{\partial y} + n^2 g \frac{q \sqrt{p^2 + q^2}}{C_o^2 h^{7/3}} \end{Bmatrix} \quad (6)$$

$g$  = acceleration due to gravity

$\rho$  = fluid density

$z_0$  = channel bed elevation

$P$  = pressure at the water surface

$n$  = Manning's roughness coefficient

$C_o$  = dimensional constant ( $C_o = 1$  for SI units and  $C_o = 1.486$  for non-SI units)

And the  $\sigma$  terms are the Reynolds stresses due to turbulence, where the first subscript indicates the direction, and the second indicates the face on which the stress acts. The pressure at the free surface is zero, and the pressure at the vessel location is related to the vessel draft as:

$$P = \rho g d \quad (7)$$

where  $d$  is the vessel draft. The Reynolds stresses are determined using the Boussinesq approach relating stress to the gradient in the mean currents:

$$\sigma_{xx} = 2\rho v_t \left( \frac{\partial u}{\partial x} \right) \quad (8)$$

$$\sigma_{yy} = 2\rho v_t \left( \frac{\partial v}{\partial y} \right) \quad (9)$$

and

$$\sigma_{xy} = \sigma_{yx} = \rho v_t \left( \frac{\partial u}{\partial y} + \frac{\partial v}{\partial x} \right) \quad (10)$$

where

$v_t$  = kinematic eddy viscosity (which varies spatially)

$u = p/h$  is the depth-averaged  $x$ -component of velocity

$v = q/h$  is the depth-averaged  $y$ -component of velocity

Values of the eddy viscosity are determined empirically as a function of the local flow variables (Rodi 1980; Chapman and Kuo 1985):

$$v_t = \frac{Cn}{h^{1/6}} \sqrt{8g(p^2 + q^2)} \quad (11)$$

where  $C$  is a coefficient that varies between 0.1 and 1.0.

## Vessel Representation

The coordinates of the vessel center  $S$  are moved during each time-step in accordance with the vessel sailing speed and direction as:

$$\mathbf{S} = \mathbf{S}_0 + \Delta \mathbf{S} \quad (12)$$

where  $\mathbf{S}_0$  is the initial location of the vessel corners, and  $\Delta \mathbf{S}$  is computed as:

$$\Delta \mathbf{S} = \begin{cases} \frac{1}{2} a t^2 & 0 \leq t \leq t_s \\ \frac{1}{2} a t_s^2 + a t_s (t - t_s) & t \geq t_s \end{cases} \quad (13)$$

where  $a$  is the specified vessel acceleration, and  $t_s$  is the time at which the vessel reaches a constant velocity ( $at_s$ ).

After the vessel center location is determined, the vessel corner coordinates are calculated from the vessel length and width. The induced pressure field resulting from the vessel draft is applied to every node within the vessel boundary, as illustrated in Figure 1. The computational mesh is constructed to apply pressure gradients across the bow, stern, and each side boundary to maintain the appropriate blockage area (vessel cross-sectional area).

## Numerical Computational Scheme

The finite element approach used is a Petrov-Galerkin formulation, which is a combination of the Galerkin test function and a non-Galerkin component to control oscillations (Berger and Stockstill 1995).

$$\sum_e \left[ \int_{\Omega_e} N_i^* \left( \frac{\partial \tilde{U}}{\partial t} + \frac{\partial \tilde{F}}{\partial x} + \frac{\partial \tilde{G}}{\partial y} + \tilde{H} \right) d\Omega_e \right] = 0, \quad \text{for each } i \quad (14)$$

where the subscript  $e$  identifies a particular element that is part of the domain  $\Omega$ , the subscript  $i$  indicates a particular test function, and the  $\sim$  symbolizes a discrete value of the variable. The finite element approximation  $\tilde{U}$  for the solution of the governing equations is given as:

$$\tilde{U} = \sum_j N_j U_j \quad (15)$$

where  $N_j$  are the bilinear basis functions and  $U_j$  are the nodal values of the solution. The Petrov-Galerkin test function, which consists of a combination of even and odd functions, is written as:

$$N_i^* = N_i \mathbf{I} + N_i' \quad (16)$$

where  $N$  is identical to the basis function,  $\mathbf{I}$  is the identity matrix, and:

$$N_i' = \beta \left( \Delta x \frac{\partial N_i}{\partial x} \hat{\mathbf{A}} + \Delta y \frac{\partial N_i}{\partial y} \hat{\mathbf{B}} \right) \quad (17)$$

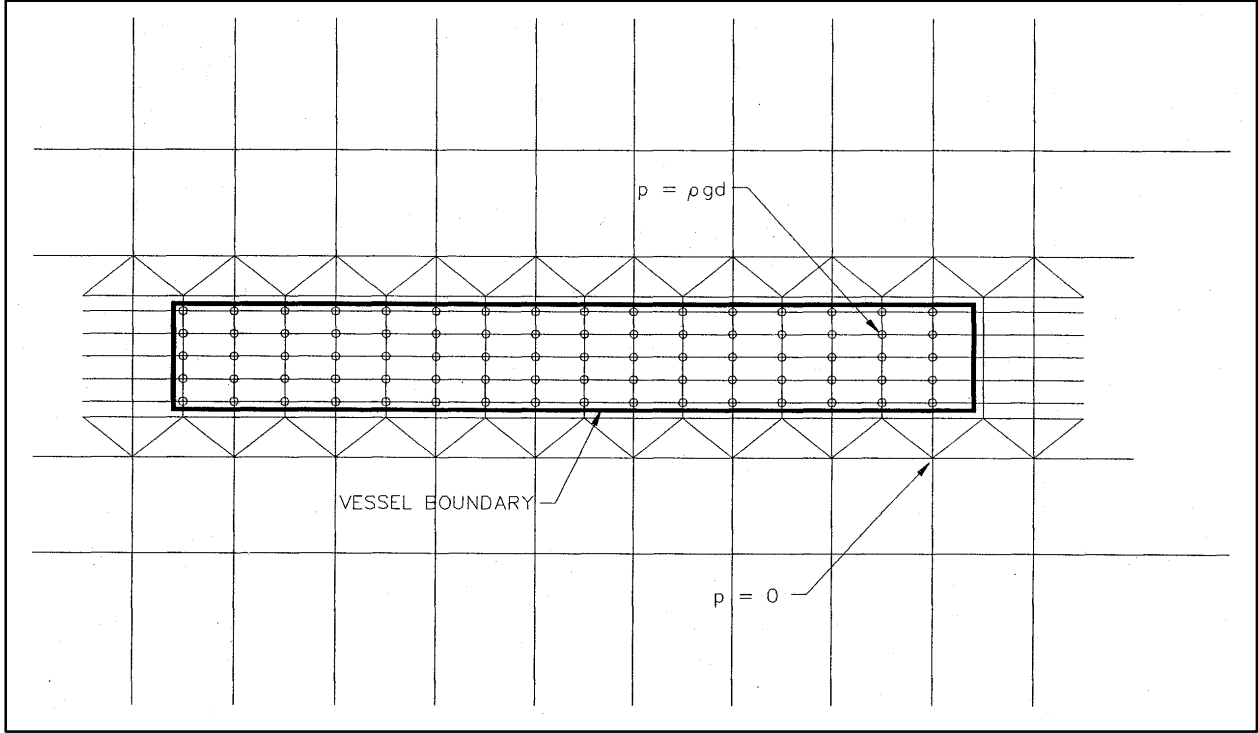


Figure 1. Discrete representation of a vessel on the numerical model computational mesh

is the stabilizing component added to the Galerkin test function. Here,  $\beta$  is a dimensionless number between 0 and 0.5,  $\Delta x$  and  $\Delta y$  are the representative element lengths (Katopodes 1986), and  $\hat{A}$  and  $\hat{B}$  are functions of the flow characteristics (Berger and Stockstill 1995; Berger 1993).

To facilitate the specification of boundary conditions, the weak form of the equations is developed using integration by parts. The weak form of the equations is given as:

$$\sum_e \left[ \int_{\Omega_e} \left( N_i^* \frac{\partial U}{\partial t} - \frac{\partial N_i}{\partial x} \mathbf{F} - \frac{\partial N_i}{\partial y} \mathbf{G} + N_i' \mathbf{A} \frac{\partial U}{\partial x} + N_i' \mathbf{B} \frac{\partial U}{\partial y} + N_i^* \mathbf{H} \right) d\Omega_e \right. \\ \left. + \oint_{\Gamma_e} N_i (\mathbf{F} n_x + \mathbf{G} n_y) d\Gamma_e \right] = 0, \text{ for each } i \quad (18)$$

where  $(n_x, n_y) = \hat{\mathbf{n}}$  is the outward unit vector normal to the boundary  $\Gamma_e$ , the symbol  $\sim$  has been omitted for clarity, and the variables are understood to be discrete values. The natural boundary conditions given in the weak statement are applied to the sidewalls to enforce no mass or momentum flux through these

boundaries. A partial slip condition is implemented at these boundaries, which allows a velocity along the wall but imposes a friction stress.

Difference equations are used to approximate the temporal derivative of the set of variables  $\mathbf{U}_j$ :

$$\left(\frac{\partial \mathbf{U}_j}{\partial t}\right)^{k+1} \approx \frac{(1 + \alpha)}{2\Delta t} (\mathbf{U}_j^{k+1} - \mathbf{U}_j^k) + \frac{(1 - \alpha)}{2\Delta t} (\mathbf{U}_j^k - \mathbf{U}_j^{k-1}) \quad (19)$$

where  $j$  is the nodal location and  $k$  is the time-step. An  $\alpha$  equal to 1.0 results in a first-order backward difference approximation, and an  $\alpha$  equal to 2.0 results in a second-order backward difference approximation to the temporal derivative. This implicit description of the nonlinear equations is solved using the Newton-Raphson method of iteration. The derivatives comprising the Newton-Raphson Jacobian are determined analytically, and the Jacobian is updated at every iteration.